Clinical Cancer Research

Screening of Conditionally Reprogrammed Patient-Derived Carcinoma Cells Identifies ERCC3–MYC Interactions as a Target in Pancreatic Cancer

Natalya Beglyarova[1], Eugenia Banina[1], Yan Zhou[2], Ramilia Mukhamadeeva[3], Grigorii Andrianov[3], Egor Bobrov[1], Elena Lysenko[1], Natalya Skobeleva[1], Linara Gabitova[1], Diana Restifo[1], Max Pressman[1], Ilya G. Serebriiskii[1], John P. Hoffman[1], Keren Paz[4], Diana Behrens[5], Vladimir Khazak[6], Sandra A. Jablonski[7], Erica A. Golemis[1], Louis M. Weiner[7], and Igor Astsaturov[1]

Abstract

Purpose: Even when diagnosed prior to metastasis, pancreatic ductal adenocarcinoma (PDAC) is a devastating malignancy with almost 90% lethality, emphasizing the need for new therapies optimally targeting the tumors of individual patients.

Experimental Design: We first developed a panel of new physiologic models for study of PDAC, expanding surgical PDAC tumor samples in culture using short-term culture and conditional reprogramming with the Rho kinase inhibitor Y-27632, and creating matched patient-derived xenografts (PDX). These were evaluated for sensitivity to a large panel of clinical agents, and promising leads further evaluated mechanistically.

Results: Only a small minority of tested agents was cytotoxic in minimally passaged PDAC cultures *in vitro*. Drugs interfering with protein turnover and transcription were among most cytotoxic. Among transcriptional repressors, triptolide, a covalent inhibitor of ERCC3, was most consistently effective *in vitro* and *in vivo* causing prolonged complete regression in multiple PDX models resistant to standard PDAC therapies. Importantly, triptolide showed superior activity in MYC-amplified PDX models and elicited rapid and profound depletion of the oncoprotein MYC, a transcriptional regulator. Expression of ERCC3 and MYC was interdependent in PDACs, and acquired resistance to triptolide depended on elevated ERCC3 and MYC expression. The Cancer Genome Atlas analysis indicates ERCC3 expression predicts poor prognosis, particularly in CDKN2A-null, highly proliferative tumors.

Conclusions: This provides initial preclinical evidence for an essential role of MYC–ERCC3 interactions in PDAC, and suggests a new mechanistic approach for disruption of critical survival signaling in MYC-dependent cancers. *Clin Cancer Res; 22(24); 6153–63. ©2016 AACR.*

Introduction

Pancreatic ductal adenocarcinoma (PDAC) affects 44,000 individuals yearly in the United States (1). This cancer is almost universally lethal, with chemotherapy having very limited efficacy and the vast majority of all diagnosed patients not surviving past the 5-year mark (1). The typical absence of drug-amenable oncogenic drivers in PDAC (2, 3) and the shortage of models representing clinical PDAC both contribute to the challenge of improving the *status quo*. Careful microdissection of PDAC tumors coupled with genomic analysis has shown that in addition to near universal mutations in KRAS and TP53, and common mutations affecting other regulators of cell cycle, such as CDKN2A (2, 3), deletions, amplifications, and mutations affecting transcriptional and chromatin remodeling, genes are important contributors to the mechanism of PDAC carcinogenesis (4). Among PDACs, the worst outcome is associated with MYC amplification, which has been detected in as many as 14% [provisional The Cancer Genome Atlas (TCGA), *cbioportal.org* (5)] to 30% (6) of these cancers.

Although targeted therapies have greatly improved response in some tumor types (7), evaluation of novel targeted agents in clinical trials for PDAC has typically been discouraging. Treatments such as the antiangiogenic agent bevacizumab (8), the Sonic Hedgehog (Shh) inhibitor vismodegib (9), or the EGFR receptor-targeting agent cetuximab (10) produced partial responses or limited stable disease in some individuals, but no statistically significant improvements in the general population of PDAC patients. With 30 to 41 new drugs granted FDA approval

[1]Program in Molecular Therapeutics, Fox Chase Cancer Center, Philadelphia, Pennsylvania. [2]Biostatistics and Bioinformatics Facility, Fox Chase Cancer Center, Philadelphia, Pennsylvania. [3]Department of Biochemistry, Kazan Federal University, Kazan, Russian Federation. [4]Champions Oncology, Baltimore, Maryland. [5]EPO Experimental Pharmacology and Oncology GmbH, Berlin, Germany. [6]Nexus Pharma, Langhorne, Pennsylvania. [7]Lombardi Comprehensive Cancer Center, Georgetown University, Washington, DC.

Note: Supplementary data for this article are available at Clinical Cancer Research Online (http://clincancerres.aacrjournals.org/).

Corresponding Author: Igor Astsaturov, Fox Chase Cancer Center, 333 Cottman Avenue, Philadelphia, PA 19111. Phone: 215-214-3971; Fax 215-728-3639; E-mail: igor.astsaturov@fccc.edu

doi: 10.1158/1078-0432.CCR-16-0149

Translational Relevance

There are few effective therapies for pancreatic adenocarcinoma, which remains one of the most lethal cancers. This work provides preclinical evidence for transcriptional vulnerability in pancreatic ductal adenocarcinoma via ERCC3 targeting. Our study revealed that a subset of pancreatic adenocarcinoma harboring amplified MYC oncogene may be highly sensitive to ERCC3 inactivation with triptolide, which provides the basis for the clinical use of triptolide-like compounds. We also demonstrate that ERCC3 expression may be a novel prognostic indicator, and suggests a new mechanistic approach for disruption of MYC in PDAC and other cancers.

each year for cancer therapy (7), there has been a notable lack of progress in pancreatic cancer, with only four new agents becoming available to the patients in the past 20 years. These include gemcitabine (11); erlotinib (12) and nab-paclitaxel (ref. 13; both used in combination with gemcitabine); and the topoisomerase 1 inhibitor irinotecan, used in combination with fluorouracil and oxaliplatin (FOLFIRINOX; ref. 14), or with fluorouracil and nanoliposomal irinotecan (15). These last approaches have increased median survival to almost 1 year (14), in contrast to the prior 6.8 months with gemcitabine, but this outcome is still dismal.

A particular limitation of identifying new effective options for pancreatic cancer is the poor correlation of drug activity between long-term cultured cell line or xenograft models and that seen in clinical trials (16). Recent efforts to establish patient-derived xenograft (PDX) models, coupled with avoidance of *in vitro* passaging, have improved the correspondence observed between the antitumor activity of drugs in mouse models and in patients (17). Particularly, as the cost of PDX models limits their availability for high-throughput screening, the matching of PDX models with minimally cultured cells derived from genotypically matched primary tumors increases flexibility in drug screening, allowing better prioritization of drug potency before subsequent *in vivo* testing. Here, we used rapidly cultured, early passage PDAC cells from 6 patients to establish patterns of chemosensitivity to 866 clinical drugs. We subsequently validated the most promising drugs *in vivo* using PDAC PDX models, many derived from the same genotyped patients as used for the screening steps. As described below, this screening identified triptolide, an irreversible inhibitor of transcription that acts through binding to the ERCC3 helicase (18), as one of the most potent PDAC growth-inhibitory compounds *in vivo* in multiple PDX models, particularly in those with MYC amplification. Exploration of the mechanism of interactions between triptolide, MYC, and ERCC3 suggests a model in which some PDACs depend on integrated MYC-ERCC3–dependent transcription, providing a therapeutic vulnerability.

Results

Chemical genomics for systematic assessment of drug activity in PDAC

To identify potential new targets and mechanisms that could be effective for the treatment of pancreatic cancer, we conducted a systematic analysis of drug sensitivity. For this purpose, we developed a representative panel of PDAC cells rapidly expanded from primary tissue *in vitro* on a layer of irradiated feeder fibroblasts in the presence of Rho kinase inhibitor Y-27632 (19, 20). This methodology provided unselected cultures of PDAC cells within 36 to 61 days after initial tissue dispersal (Fig. 1A; Supplementary Fig. S1A), thus avoiding cell identity changes imposed by *in vitro* culture (21) while producing numbers of primary cells sufficient for drug sensitivity testing. We derived cultures of PDAC cells from primary surgical tumor samples taken directly from patients (3 cases), or from first passage PDAC xenografts implanted to the flanks of immune-deficient *C.B17-scid* mice (3 cases). These approaches yielded predominantly epithelial carcinoma cell populations, as judged by cellular morphology (Supplementary Fig. S1B), keratin expression, and the absence of reactivity with mouse-specific antibody or low to absent amplification of the mouse Alf gene by genomic qPCR (Supplementary Fig. S1C). The PDX models and the derived cellular cultures carried mutations identical to the patient's tumors (Supplementary Table S1).

Our goal was to generate results we could rapidly translate to the clinic for the treatment of PDAC. Therefore, we systematically probed chemosensitivity of the *in vitro* PDAC models using both a focused library of 866 drugs from the NCI Clinical Collection (NCC; refs. 22, 23) and the FDA-approved drug collection (Supplementary Table S2). These drugs have been already tested in clinical trials for numerous oncologic and nononcologic indications, and have desirable drug-like properties including bioavailability, stability, and a well-characterized safety profile. We used the AUC as the most objective parameter of drug activity (24) which could be enumerated in all tested compounds. Drug cytotoxicity against PDAC cells was assessed at 6 therapeutically achievable concentrations ranging from 16 nmol/L to 10 μmol/L, using a CellTiterGlo viability assay measuring cellular ATP in rapidly expanded PDAC cell cultures from 6 patients (in 8 screens in total; Supplementary Table S2). To ascertain the reproducibility of the screen data, we independently derived parallel cell cultures from two separate sources: for patient 1, we cultured two first passage xenografts; for patient 15, we derived independent cultures from the primary tumor and the passage 1 xenograft. In both cases, we found highly correlated patterns of chemosensitivity between the biological replicates (Supplementary Fig. S1D).

Of the chemotherapy drugs that registered as the most potent agents in this assay (Fig. 1B), there was little variability in rank for growth inhibition between the 6 independent patient-derived cell cultures. Notably, the most potent drugs (Fig. 1B) included 5 anthracycline antibiotics (idarubicin, doxorubicin, epirubicine, mitoxantrone, and actinomycin D) which are known as transcriptional repressors based on their primary activity in binding the DNA minor groove (25). These also included a histone deacetylase (HDAC) inhibitor, romidepsin, which is involved in chromatin remodeling and transcription (26), and triptolide, a selective irreversible inhibitor of the transcriptional regulator ERCC3 [also known as xeroderma pigmentosum group B (XPB), a helicase in the TFIIH protein complex (18); Fig. 1B]. Together, DNA-targeting drugs comprised 8 of the 10 most potent hits.

Among the top 15% of most active compounds in PDAC screening (using an AUC threshold of 3), we subclassified drugs based on their described principal mechanisms of activity. Among those, drugs interfering with protein synthesis (homoharringtonine, HHT), folding (HSP90 inhibitor ganetespib), or degradation (proteasomal inhibitors) showed the greatest cytotoxicity

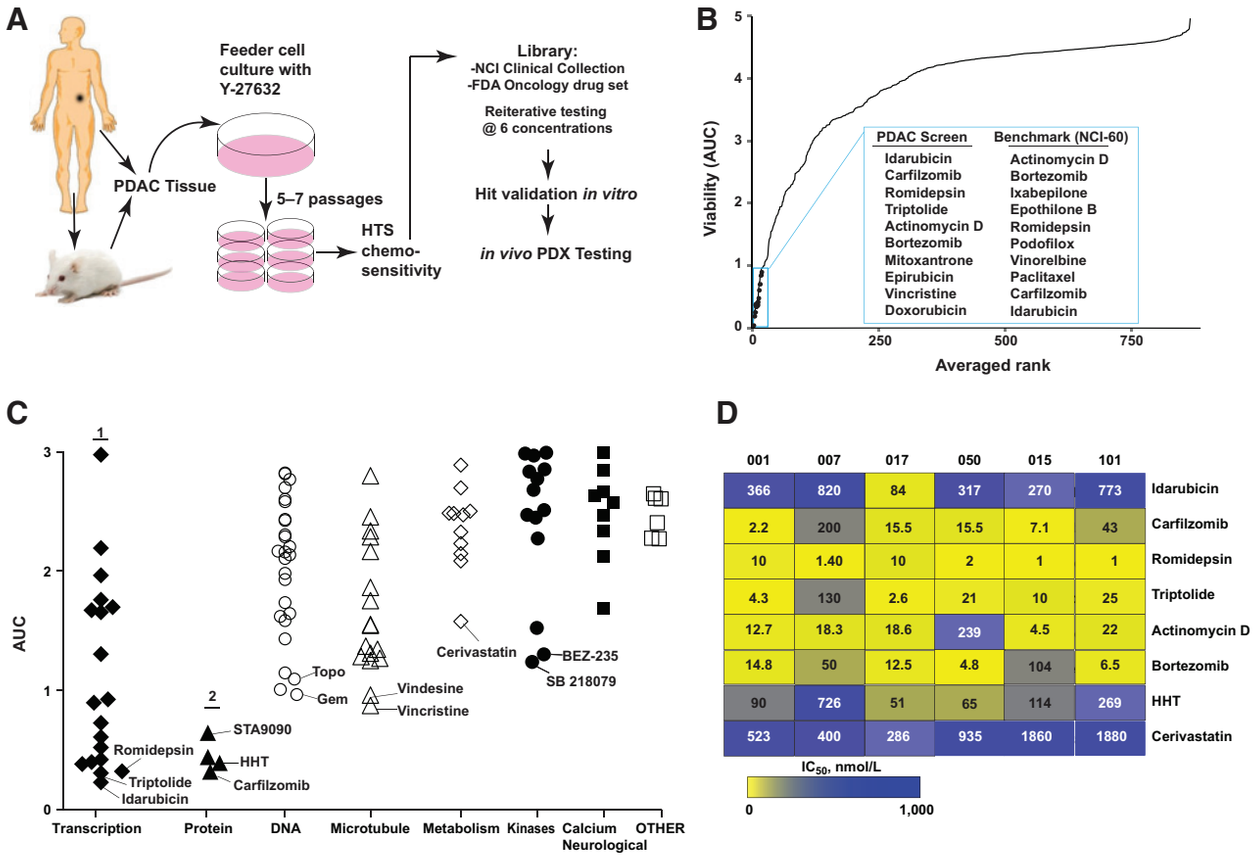

Figure 1.

Rapidly derived PDAC cells for *in vitro* drug sensitivity testing. **A,** Schema of the procedure. Pancreatic carcinoma cells obtained from the surgical or the first passage patient-derived xenograft tissues were grown with irradiated fibroblasts for 30 to 61 days and used for robotic high-throughput cytotoxicity testing. **B,** Rank order of cytotoxicity estimated as the AUC of viability dose–response curve at drug concentrations ranging from 16 nmol/L to 10,000 nmol/L. *Insert*, Top 10 cytotoxic drugs in the PDAC screen and NCI-60 panel. **C,** Functional classes of the active drugs in the primary screen. Shown is averaged AUC obtained in 6 early passage pancreatic adenocarcinoma cultures (AUC cutoff $\leq$3). PR, protein synthesis, folding, and degradation inhibitors; TR, transcriptional repressors; DNA, DNA-damaging drugs; MT, microtubular toxins; MET, metabolic inhibitors; KI, kinase inhibitors; CB/NEU, calcium channel and neurotransmitter interfering drugs; other, unclassified drugs. **D,** The *in vitro* validated IC_{50} (inhibitory concentration, nmol/L) for top screen hits.

in vitro (Fig. 1C). Among transcriptional repressors, triptolide and epirubicin had the greatest activity against PDAC cells *in vitro*. Microtubule poisons (MT) and drugs directly damaging DNA (DNA) were of substantially lower potency, potentially reflecting a limited single-agent activity of these drugs against pancreatic cancer.

To determine if the hits we observed were uniquely active in PDAC, we benchmarked the cytotoxicity profile we generated in the PDAC cell models to public data reporting systematic analyses of drug chemosensitivity for NCI-60 panel of cell lines (27) which are available in CellMiner (28, 29). The NCI-60 panel does not include PDAC cell lines. Of 189 drugs in common between the 866 compound library we screened directly, and those tested against the NCI-60 panel, 156 had cytotoxicity of greater than 30% (IC30; Supplementary Fig. S2A) relative to vehicle. Using viability ranking to normalize between the data sets, unsupervised clustering analysis determined that rapidly cultured PDAC cells differed distinctly in chemosensitivity pattern from the NCI-60 panel (Supplementary Fig. S2B). Compounds most active in both the NCI-60 analysis and PDAC screen included two proteasome inhibitors (bortezomib and carfilzomib), an anthracycline (actinomycin D), and romidepsin (Fig. 1B). Contrastingly, the ERCC3 inhibitor triptolide and other transcriptional inhibitors were among the top most potent cytotoxins in the PDAC screen but not in the NCI-60 panel.

To nominate candidates for further exploration *in vivo*, we further validated the IC_{50} values for selected drugs representing these mechanistic classes in six patient-derived cell lines (Fig. 1D), selecting five candidates (romidepsin, triptolide, carfilzomib, bortezomib, and homoharringtonine) for further validation in PDX models.

Identification of a potent activity of triptolide *in vivo*

We benchmarked these selected agents against a set of chemotherapy drugs currently approved by the FDA (www.NCCN.org) for the treatment of pancreatic cancer, albeit with relatively limited clinical activity. At 21 days, single-agent treatments with gemcitabine, 5-fluorouracil, or platinum

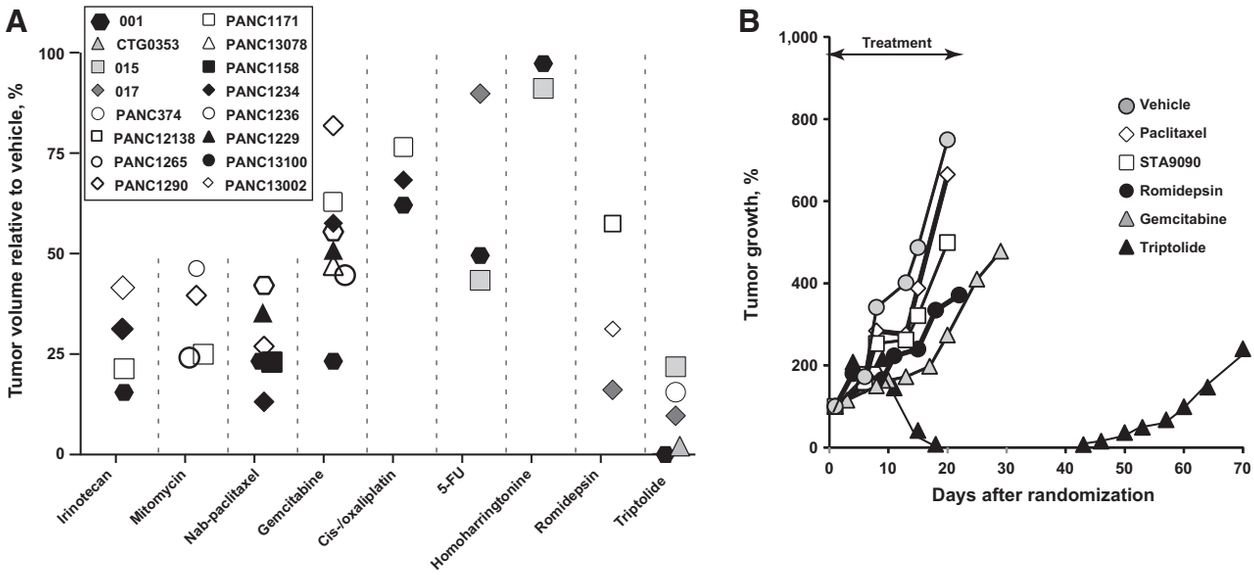

Figure 2.

Validation of screen hits in a panel of patient-derived PDAC xenografts. **A,** Efficacy of screen hits benchmarked against currently used chemotherapy against PDAC patient-derived xenografts. Data represent mean tumor volume on day 21 as percentage of vehicle, $n \geq 5$ tumor in each treatment group per model. **B,** Superior efficacy of triptolide against pancreatic adenocarcinoma xenograft 001. Mice ($n = 5$ mice per group each grafted in both flanks) were treated at clinically relevant doses: paclitaxel 50 mg/kg i.p. 3 times a week; STA9090 125 mg/kg oral daily; romidepsin 2.31 mg/kg i.p. on days 1, 5, and 9; gemcitabine 100 mg/kg i.p. once weekly; and triptolide 0.2 mg/kg oral daily for 21 days. Tumor sizes were measured twice weekly and expressed as a percentage of the initial tumor volume on day 1. Shown are averaged tumor volumes.

agents caused approximately 50% growth delay of multiple pancreatic PDX models *in vivo*; nab-paclitaxel, mitomycin C, and irinotecan showed stronger (~75%) tumor growth suppression (Fig. 2A and Supplementary Fig. S3A). Among the new candidate compounds, romidepsin (targeting HDAC-1 and -2) also caused approximately 75% growth delay of PDX tumors (Fig. 2A and Supplementary Fig. S3B) at MTDs (26). Homoharringtonine, a plant alkaloid and a ribosomal inhibitor used for the treatment of chronic myeloid leukemia (30), was inactive *in vivo* (Fig. 2A), as was carfilzomib (Supplementary Fig. S3C). The proteasome inhibitor bortezomib produced only a transient growth delay *in vivo* (Supplementary Fig. S3C), in accord with the negative outcome of a randomized clinical trial of bortezomib in combination with gemcitabine in metastatic pancreatic cancer (31).

In contrast, triptolide given orally at daily doses of 0.2 mg/kg for 21 days (32) showed the highest activity against 5 PDX pancreatic cancer models tested (~90%; Fig. 2A) and in 2 cases, caused durable complete responses after cessation of dosing (Fig. 2B). This caused us to focus further analysis on this compound.

Functional interactions of MYC and ERCC3 in pancreatic cancer

Testing of triptolide in conditionally reprogrammed PDAC cells revealed variable sensitivity between lines (Fig. 3A). More sensitive PDAC cells exhibit rapid induction of apoptosis after 24 hours in the presence of low nanomolar concentrations of the drug (Fig. 3B). Triptolide inhibits transcription by binding to ERCC3, a component of the TFIIH transcription complex (18, 33). We assessed global mRNA expression in 001 PDAC cells 6 hours after treatment with triptolide versus vehicle (Supplementary Fig. S4). We ranked the gene transcripts based on the fold change in their abundance in triptolide-treated PDAC 001 cells (Supplementary Fig. S4A and S4B). We further benchmarked the triptolide-dependent mRNA change in 001 cells against mRNA expression data for 9 cancer cell lines treated with triptolide for 6 hours, available through the NIH LINCS resource (34). Analyses of significantly downregulated gene transcripts in both the PDAC 001 and LINCS datasets showed MYC oncogene as a triptolide target among several Cancer Census genes affected (Supplementary Fig. S4C; Supplementary Table S3). In keeping with previously reported depletion of short-lived mRNA including MYC in A549 lung cancer cells treated with triptolide (35), we determined rapid downregulation of MYC mRNA (Fig. 3D) and protein (Fig. 3E) following triptolide treatment. MYC levels were undetectable after 1 hour of incubation with 50 nmol/L triptolide in the highly sensitive PDAC 001 and 017 cells. Triptolide dose titration experiments showed marked loss of MYC expression at concentrations as low as 6 nmol/L in 001 and 017 cells, but not in relatively refractory 015 and 007 cells (Fig. 3F; Supplementary Fig. S5A), at 24 hours after dosing. Triptolide effects on MYC depletion markedly greater than that of other established transcriptional repressors such as actinomycin D, romidepsin, and idarubicin (Supplementary Fig. S5B). MYC phosphorylation on T58 and S62 has been previously shown to increase MYC protein stability and contribute to KRAS-driven carcinogenesis (36). Emphasizing the relationship between triptolide response and short mRNA and protein turnover of the majority of cellular MYC, triptolide caused little change in the levels of T58- and S62-phosphorylated MYC protein. As expected for a transcriptional repressor (37, 38), we also observed that activity of triptolide induced the rapid decay of the RNA polymerase II subunit RPB1, and the dose- and time-dependent loss of phosphorylation of

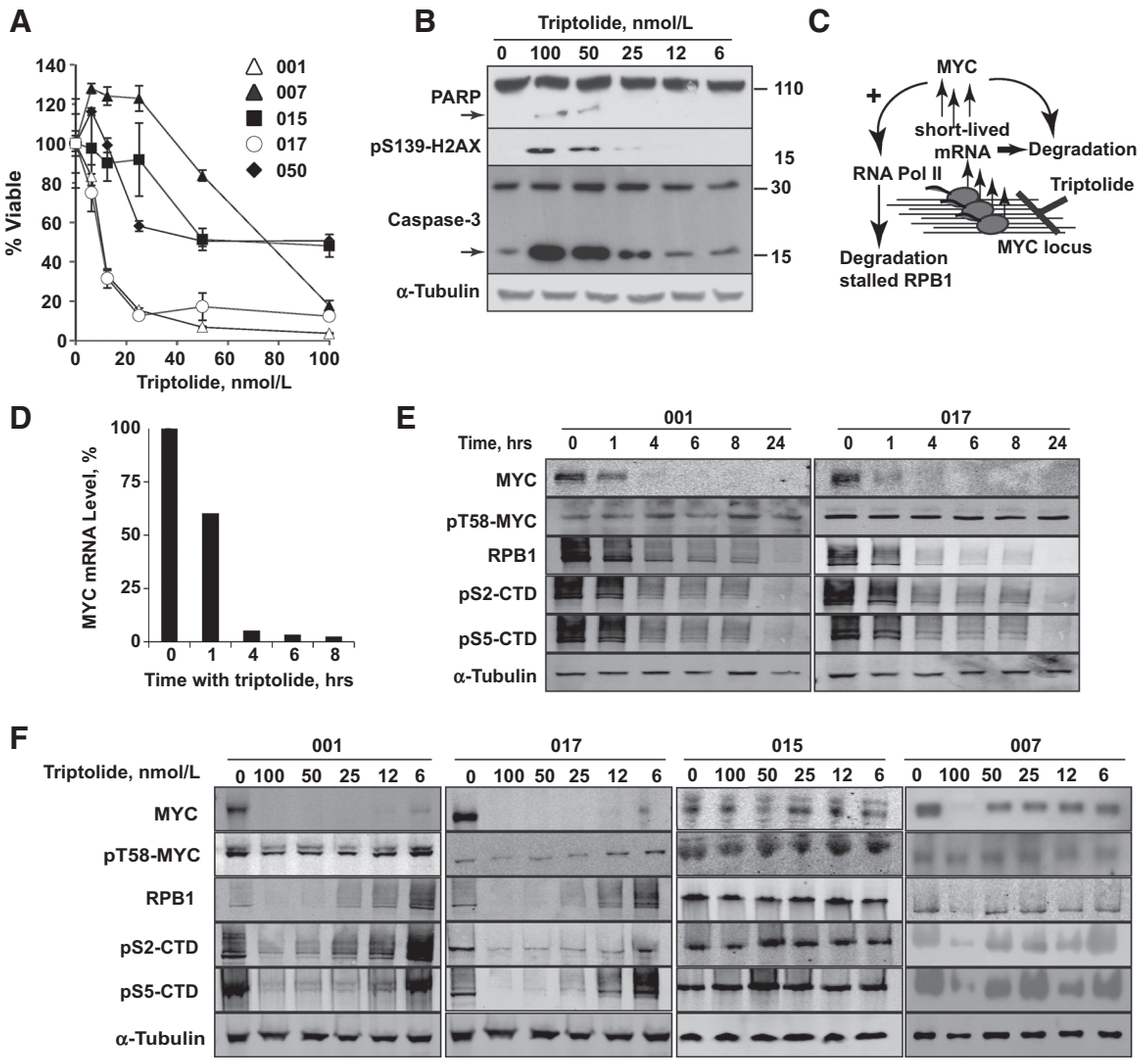

Figure 3.

Inactivation of oncogenic transcription with triptolide targets MYC. **A,** Sensitivity of the early passage PDAC cells to triptolide. Data represent mean ± SD of 3 repeats. **B,** Triptolide induces apoptosis. Shown are lysates of 017 cells treated overnight with the indicated concentrations of triptolide. *Arrows*, proteolytic fragments of PARP (p89) and caspase 3. **C,** Proposed model for triptolide-mediated inactivation of RNA Pol II transcription and MYC depletion. **D,** Rapid depletion of MYC mRNA in PDAC cells 001 treated with triptolide at 100 nmol/L as assessed by qRT-PCR. **E,** Triptolide at 50 nmol/L causes rapid depletion of MYC and RPB1 in sensitive PDAC cells 001 and 017. **F,** Differential effect of triptolide on MYC expression in sensitive (001 and 017) versus resistant (015 and 050) PDAC cells at 24 hours as assessed by Western blot.

serines S2 and S5 in the RPB1 C-terminal heptapeptide repeat (ref. 39; Fig. 3F; Supplementary Fig. S5A). The levels of structural proteins such as alpha-tubulin and beta-actin were unaffected by triptolide treatment.

Mechanisms of PDAC sensitivity and resistance to triptolide

We next determined whether the endogenous expression of MYC or ERCC in PDAC models predicted their susceptibility to triptolide. Direct comparison of MYC protein levels in early passage PDAC cultures showed significant variability between lines, with the highest levels observed in two *in vitro* sensitive 001 and 017 cells, whereas the levels of ERCC3 were nearly similar across all models tested (Fig. 4A). Further, overexpression of exogenous MYC using rapid lentiviral transduction and puromycin selection conferred 2- to 5-fold increase in sensitivity to triptolide. The drug-sensitizing effect of MYC overexpression was especially prominent in PDAC cells 050 which are triptolide refractory suggesting a direct relationship of MYC status with triptolide response (Fig. 4B). Contrastingly, overexpression of the triptolide target ERCC3 conferred resistance to 2 most sensitive (001 and 017) out of 3 PDAC cells, supporting a direct on-target effect of triptolide (Fig. 4B and Supplementary Fig. S6A). In contrast, expression of neither MYC nor ERCC3 affected PDAC cells sensitivity to EZH2 histone methyltransferase inhibitor UNC1999 (Supplementary Fig. S6B), indicating specific interaction with triptolide.

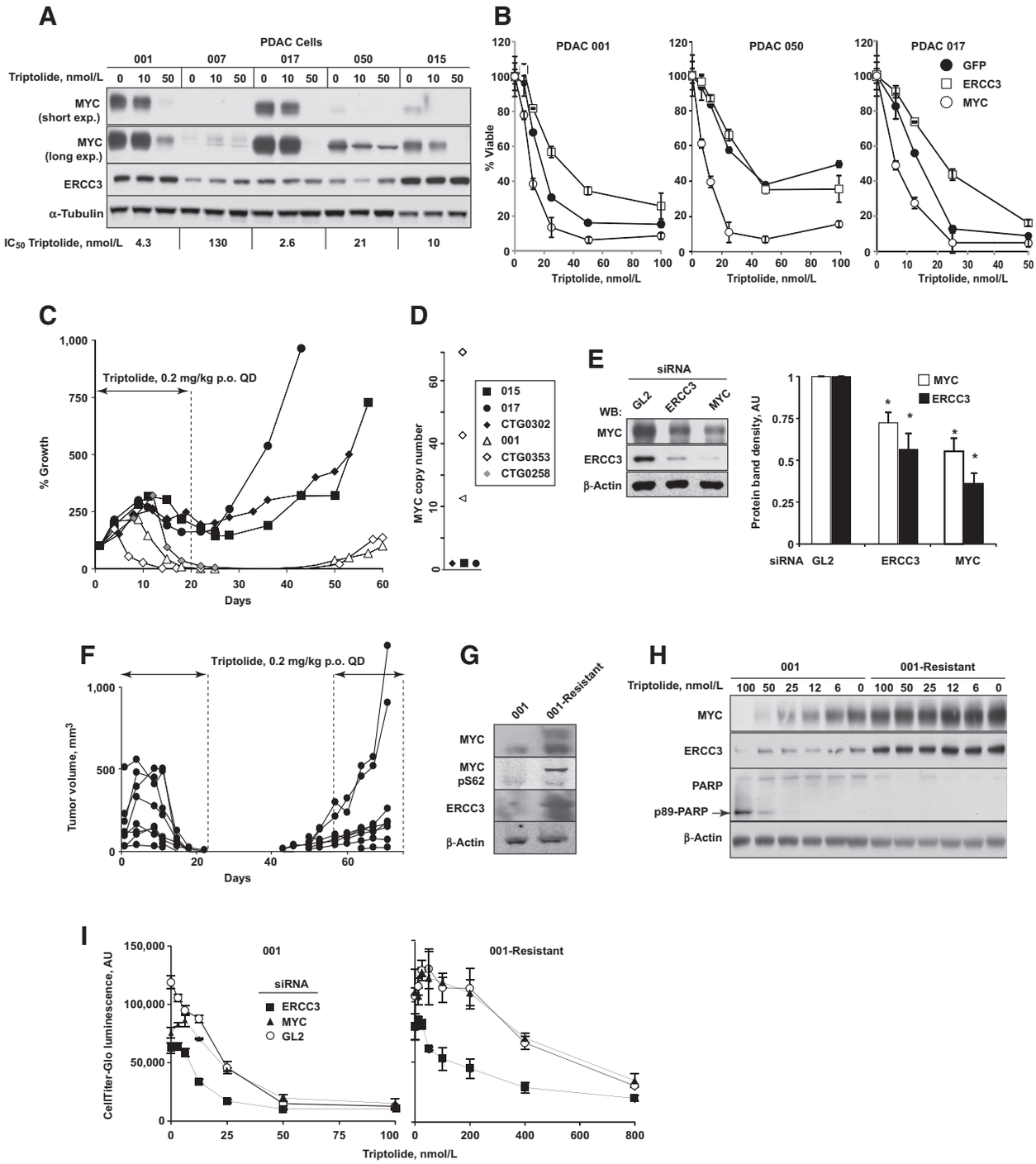

Figure 4.

MYC and ERCC3 exert opposing effects on PDAC sensitivity to triptolide. **A,** Increased MYC expression and depletion in triptolide-sensitive PDAC cells 001 and 017. IC_{50} values for each cellular model are indicated above the Western blot. Cells were treated with indicated triptolide concentrations overnight. **B,** Lentiviral expression of MYC increases PDAC cells sensitivity to triptolide in contrast to ERCC3, which conferred triptolide resistance to 001 cells. **C,** Complete responses to triptolide in MYC-amplified xenografts. **D,** MYC gene copy number by genomic qPCR. *Closed symbols,* PDX models with normal MYC gene copy number; *open symbols*, MYC-amplified. **E,** Coregulation of MYC and ERCC3 expression in 001 cells. Cells were transfected with 50 nmol/L of indicated siRNA, proteins were analyzed in 48 hours by Western blot (left). Right, averaged results of three independent experiments. *, paired *t* test $P < 0.05$ compared with siGL2 control. **F,** Tumor volumes of PDAC 001 over time show initial complete response and recurrence during a drug-free interval with acquired resistance in some tumors. **G,** Increased MYC and ERCC3 expression in lysates of triptolide-resistant recurrent PDAC 001 tumors. **H,** The *in vitro* expanded triptolide-resistant 001 cells maintained high level of ERCC3 and MYC expression and resist apoptosis as indicated by PARP fragmentation. **I,** Silencing of ERCC3 reverses acquired triptolide resistance in 001-R cells. Cells were transfected with 50 nmol/L of siRNA, and treated with triptolide in 24 hours. Viability was measured by CellTiter-Glo luminescence in 96 hours after seeding. p.o., orally; QD, once daily.

The effect of triptolide *in vivo* on the growth of pancreatic xenografts was highly variable (Fig. 4C) from rapid complete responses to transient growth delay. We further probed the relationship of MYC genomic copy number to the PDAC sensitivity to triptolide based on the established MYC addiction in MYC-amplified cancers (40). Of all PDAC models, only tumor tissue of patient 001 was MYC-amplified and carried 12 copies of MYC gene by comparative genomic hybridization and genomic qPCR (Fig. 4D). Thus, we additionally tested two chemotherapy-refractory PDX models, gastric (CTG0353) and ovarian (CTG0258), with high levels of MYC amplification (with 42 and 70 copies of MYC gene, respectively; Fig. 4D). Oral administration of triptolide for 21 days in all three MYC-amplified PDX models demonstrated complete regression of all tumors (Fig. 4C). Contrastingly, pancreatic or other PDX models with a normal copy number of MYC (015, 017, and CTG0302) showed regression but no complete responses, and tumors resumed growth after the triptolide treatment stopped. In contrast to the high sensitivity to triptolide in the short-term culture (Fig. 3A), PDAC 017 xenografts carrying diploid MYC gene showed only transient growth delay (Fig. 4D).

To further investigate the dependence of MYC on ERCC3 function and to rule out a potential off-target activity of triptolide, we silenced ERCC3 with siRNA and measured MYC expression. Interestingly, depletion of ERCC3 significantly reduced MYC protein expression (by 30%; Fig. 4E), and MYC-silenced 001 cells markedly downregulated ERCC3 protein (at 50%; Fig. 4E). Extending this latter result, we used a tetracycline repressor-regulated model of MYC expression (41) to confirm that MYC suppression led to loss of ERCC3 protein expression (Supplementary Fig. S6C), suggesting a reciprocal dependency of MYC and ERCC3 to regulate oncogenic transcription.

PDACs acquire resistance to triptolide via increased ERCC3 and MYC

Despite the dramatic initial meltdown of MYC-amplified tumors following a 21-day course of triptolide treatment, in most animals, the tumors recurred after a prolonged remission (Fig. 4C and F). Re-treatment of the recurrent tumors with the same dose of triptolide caused regression of all but a few tumors, which grew in the presence of the drug. Remarkably, the resistant tumor showed markedly upregulated expression of ERCC3 and MYC (Fig. 4G), which is consistent with our proposed model of a critical dependency between ERCC3 and MYC. Triptolide-refractory 001 cells obtained from the refractory tumors grew in the presence 50 nmol/L triptolide, whereas the naïve 001 cells experienced complete growth inhibition at approximately 5 nmol/L (Fig. 1D). This acquired triptolide resistance was selective, as sensitivity to the BRD4 inhibitor JQ1 and UNC1999 was comparable in triptolide-sensitive and -refractory cells (Supplementary Fig. S6D and S6E).

Previous reports had indicated that inactivating mutations in ERCC3 or GTF2H4 confer triptolide resistance (33, 42). We ruled out such acquired mutations by sequencing the RNA from resistant cells, finding no mutations in any components of the TFIIH or RNA polymerase II complex (Supplementary Fig. S7). However, these triptolide-refractory 001 cells had markedly increased levels of ERCC3 and were resistant to triptolide-mediated MYC depletion (Fig. 4C). Furthermore, silencing ERCC3, but not MYC, reversed the triptolide resistance (Fig. 4D), indicating that overexpression of drug target is responsible for the acquired resistance. These findings are also consistent with the results of ERCC3 overexpression (Fig. 4B).

ERCC3 expression interacts with CDKN2A deletion to predict PDAC patient survival

Our data suggested that ERCC3 expression, like MYC expression, might be related to survival in PDAC patients. Using the survival information from the TCGA dataset (cbioportal.org; refs. 2, 43), we determined that PDAC with high ERCC3 expression had significantly worse overall survival (OS; median of 13.8 vs. 16.8 months; log-rank test $P = 0.029$; Fig. 5A). ERCC3 expression was independent of the MYC copy-number status of the tumors (Pearson 0.067). We then examined whether the predictive value of ERCC3 expression was influenced based on tumor genotype, again using data from *cbioportal.org* and querying a set of common genetic lesions in PDAC. Genetic loss of CDKN2A, encoding p16, is common in PDAC and associated with deregulation of cell-cycle control (2, 3). Although homozygous deletions of CDKN2A did not independently predict OS (Fig. 5B), this genotype has a striking interaction with ERCC3 expression. Elevation of ERCC3 strongly predicted shorter OS in CDKN2A-null tumors (Fig. 5C, median of 4.8 vs. 19.9 months; log-rank test $P = 0.005$), but lost predictive power in CDKN2A wild-type tumors (Fig. 5D).

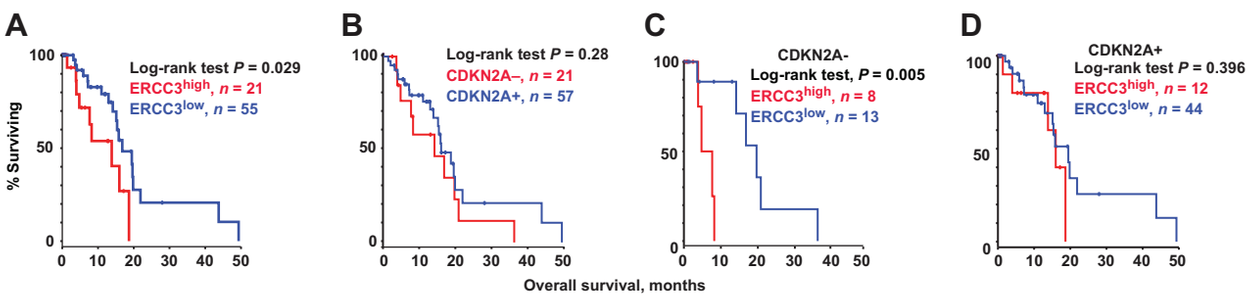

Figure 5.

Effect of ERCC3 expression on survival of patients with PDAC. **A,** Effect of ERCC3 mRNA expression on PDAC survival using ERCC3 > 0.6 as high expression threshold from the TCGA dataset (2). Homozygous deletion of CDKN2A alone (**B**) has no effect on survival. Patients with $ERCC3^{high}$ and homozygous deletion of CDKN2A had significantly worse survival (**C**) compared with no effect of ERCC3 expression in CDKN2A-positive PDAC (**D**).

Discussion

Taken in sum, our data demonstrate in multiple PDX and cell culture models for PDAC that inhibition of ERCC3 with triptolide is a useful therapy, particularly in the context of amplified or overexpressed MYC. They also demonstrate specific interaction between ERCC3 and MYC, reflecting interdependent protein expression required for cell viability and resistance to triptolide. Together, these results suggest the idea that inhibition of the transcription factor ERCC3 is particularly important in fast-proliferating cells and tumors lacking growth restriction checkpoints: an idea further supported by our identification of a relationship between high ERCC3 expression and poor overall survival for PDAC, particularly in the context of a common CDKN2A gene disruption. Our data thus imply triptolide, in addition to MYC-amplified carcinomas, may also be particularly effective in the subset of PDAC with CDKN2A deletions.

This study, for the first time, used a recently described rapid culture method with limited passaging (19, 20) to develop tools for the evaluation of PDAC chemosensitivity in physiologic models. Subsequent screening with these tools evaluated many distinct pharmacologic drug classes in the currently available pharmacopeia. This emphasized a particularly high sensitivity to agents targeting the transcriptional apparatus and protein turnover, some of which were comparable to or outperformed conventional chemotherapy drugs currently in use for PDAC. Not all of these agents were effective in subsequent *in vivo* testing: For instance, homoharringtonine (also known as omacetaxine mepesuccinate) showed lower activity *in vivo* than *in vitro*. This may reflect the lower proliferation index of tumors growing in desmoplastic microenvironments, relative to the more exponential growth conditions pertaining in cultured cells, which reduces absolute dependence on maximally efficient mRNA and protein expression. Alternatively, it may reflect poor penetration of the drug in tumor tissue, a limiting factor for some otherwise promising compounds. However, the ERCC3-targeting drug triptolide was highly effective *in vivo*, with activity strongly linked to disruption of MYC expression. This activity may reflect the irreversible modification of ERCC3 by triptolide, resulting in an inescapable brake on the core transcriptional machinery.

The transcriptional machinery has been assuming greater importance as a target of therapy in PDAC. Genomic analyses identifying common mutations in the SWI/SNF chromatin remodeling complex genes including the DNA binding subunits (ARID1A, ARID1B, PBRM1) and enzymatic subunits (SMARCA2, SMARCA4; ref. 44) emphasized the role of chromatin remodeling in PDAC etiology. The role of epigenetic mechanism was also demonstrated for the histone H3K36 demethylase KDM2B, which is overexpressed in PDAC (45). Preclinical studies targeting chromatin remodeling with a bromodomain 4 inhibitor, JQ1 (46), or with a combination of JQ1 and a HDAC inhibitor (47) have demonstrated efficacy in PDX and in a genetic mouse model of PDAC. Importantly, control of tumor growth with these therapies involved limiting activity of MYC, which is a critical promoter of pancreatic carcinogenesis (48), and for which high expression is known to be a poor prognostic factor for PDAC (4). Our data suggest further evaluation of triptolide in combination with other means to deregulate MYC as a promising approach.

By identifying regulatory cross-signaling between ERCC3 and MYC, our results will help guide the future clinical development of solubility-enhanced triptolide analogs (ClinicalTrials.gov identifier NCT01927965; ref. 32). Of particular interest, this work is the first to suggest that increased ERCC3 expression may be a hallmark of aggressive PDAC in the context of the cell-cycle deregulation associated with loss of CDKN2A. More work is required for better understanding whether ERCC3 overexpression contributes to a poor outcome based on its role in transcription, or through provision of increased resistance to the conventional DNA damaging therapies used to treat PDAC. Whatever the mechanism, this observation will also guide the clinical development of triptolide analogs.

Materials and Methods

Procurement of human pancreatic adenocarcinoma tissues

We obtained surgical pancreatic adenocarcinoma specimens from consented patients in accordance with the Fox Chase Cancer Center Institutional Review Board protocol 12-822. Tumor tissue was placed in ice-cold sterile transport medium and immediately implanted in Matrigel (Corning Life Sciences) to both flanks of C-B17.*scid* mice as described (16) and/or cultured with irradiated J2 feeder fibroblasts as detailed below. In our experience, take rate from metastatic sites was higher at 6/10 (60%), compared with the primary PDAC where implantation success was at 11/56 (19.6%).

Antibodies and reagents

The antibodies used in Western blot were pThr58-Myc (Santa Cruz Biotechnology; sc-135647), pS62-Myc (Abcam), ERCC3 (A301-337A; Bethyl Laboratories); antibodies to MYC (#5605), Rpb1-CTD (#2629), pSer2-CTD of Rpb1 (#8798), pSer2-CTD of Rpb1 (#8807), β-actin (#4967), and α-tubulin (#2125) were purchased from Cell Signaling Technology. Triptolide was purchased from Cayman Chemical and dissolved in DMSO as 1 mmol/L stock. Chemotherapy drugs were purchased from the Fox Chase Cancer Center pharmacy.

Primary cultures of pancreatic adenocarcinoma cells

Fragments of freshly obtained tumor tissues were dissociated using collagenase/hyaluronidase and Dispase (StemCell Technologies) at 37°C for 3 hours with occasional shaking as per the manufacturer's protocol. PDAC cells were then placed in flasks layered with irradiated 10^6 J2 NIH-3T3 fibroblast feeder cells in full medium. The cell culture medium included complete DMEM with freshly added supplements (GIBCO-Thermo Fisher Scientific): 10% FBS, penicillin, streptomycin and glutamine, F12 nutrient mix (all at 1X), 25 μg/mL hydrocortisone, 125 ng/mL EGF, 5 mg/mL insulin, 250 μg/mL fungizone, 10 mg/mL gentamycin, 10 μg/mL nystatin, 11.7 μmol/L cholera toxin, and 5 μmol/L Rho kinase inhibitor Y27632 (Sigma-Aldrich). The medium was replaced every 2 days. The cells were cultured for a period of 1 to 2 months and split twice a week using standard trypsinization procedure (19). Typically, 10^6 irradiated feeder J2 cells were plated at each passage with 1 to 2×10^6 PDAC cells in a T75 flask. Prior to compound screening, feeder cells were detached following a brief incubation with trypsin, which caused their rapid detachment while PDAC cells remained adherent to the flask.

Compound screening

The library included a panel of 730 compounds of the NCC (22, 23) and 101 FDA-Approved Oncology drug Set IV from NCI/DTP Open Chemical Repository (http://dtp.cancer.gov) encompassing the agents that have been in phase I–III clinical trials and are

part of the NIH Roadmap Molecular Libraries Screening Centers Network (49). Controls and several screening compounds were added to the plates manually (full list in Supplementary Table S1). PDAC cells were plated in 96-well flat-bottom plates (Sarstedt) at 2,500 cells per well 48 hours prior to adding the drugs. The compound library was maintained as 10 mmol/L stock in DMSO which has been used for further serial dilution using robotic high-throughput plate handling automation (CyBio) to create 2 replicates of each library plate at 10 μmol/L, 2 μmol/L, 0.4 μmol/L, 0.08 μmol/L, and 0.016 μmol/L final drug concentrations. Sensitivity was assessed on day 6 using standard viability assay (CellTiter-Glo, CellTiter-Blue, Promega; ref. 50).

Xenograft experiments

Cryopreserved in DMSO PDX tumor fragments were quickly thawed, washed in RPMI, and resuspended in 1:1 mix of RPMI and Matrigel (Corning Life Sciences) on ice until the moment of implantation. Tumor fragments were subcutaneously injected using 1 mL syringe and 18G $1^1/_2$ needle in both flanks of 5- to 8-week-old *C-B17.scid* mouse. Animals with established tumors (around 150 mm^3) were randomly divided to receive indicated drugs or vehicle with indicated dose schedules and routes of administration. Animals were weighed twice a week. Tumor size was measured with a digital caliper twice a week, and volumes were calculated using the modified ellipsoid formula as described (50) until the maximum size of 1,500 mm^3 or if animals exhibited distress, >20% weight loss or if tumors ulcerate, in which case mice were humanely euthanized.

Western blot

The DX tumor tissues were lysed with T-PER reagent (Thermo Fisher Scientific) containing double concentration of Halt protease and phosphatase inhibitors (Thermo Fisher Scientific). For Western blot, cells were seeded on 6-well plates at density of 30,000 cells per well in RPMI-1640 supplemented with 1% FBS, 2 mmol/L L-glutamine, 25 mg/L Insulin, and 100 mg/L penicillin/streptomycin. Next day, the cells were treated with indicated drugs for 24 hours and lysed with RIPA lysis buffer (Santa Cruz Biotechnology) containing Halt protease and phosphatase inhibitors (Thermo Fisher Scientific). Protein concentrations were measured using BSA assay. Western blot membranes were scanned using Odyssey infrared imaging reagents including blocking buffer and secondary antibodies (LI-COR).

Quantitative PCR and transfections

We used the Human Multicopy Reference assay (QIAGEN) to determine *MYC* gene copy number by qPCR in PDAC cells using an ABI Prism 7700 Detection System (Applied Biosystems) with the following primers: *MYC*, forward-TTCTAACAGAAATGTCCTGAGCAATC, reverse- TCAAGACTCAGCCAAGGTTGTG; *ALB* (albumin), forward-CATTTATTGGTGTGTCCCCTTG, reverse-ACACCAGTGAAAACAATTTAAGCC. The results were analyzed by the comparative *Ct* method to establish relative expression curves. *MYC* copy number was quantified relative to *ALB* based on the relative stability of ALB chromosomal locus 4q11-q13 in PDAC (3). PDAC cells were transfected with validated siRNA at 50 nmol/L concentrations targeting human MYC (CTCGGTGCAGCCGTATTTCTA) and ERCC3 (CCGGTTCACCTCCGATGCCAA) genes and the firefly luciferase GL2 (AACGTACGCGGAATACTTCGA) as a non–targeting-negative control in triplicates with siRNA mixed with HiPerFect Transfection Reagent (QIAGEN) according to the manufacturer's reverse-transfection protocol. For ERCC3 overexpression in HEK-293 cells, the full-length ERCC3 cDNA was amplified using forward-ATGGGCAAAAGAGACCGAGCG and reverse-CTCTTCAAGCGCTTTAGGAAATGA primers and Gateway-cloned to pLEX mammalian expression vector (OHS4735, Thermo Scientific). Cells were transfected with plasmid DNA using Lipofectamine 2000 as per the manufacturer's (Thermo Scientific) protocol. For lentiviral expression, full-length cDNA of ERCC3 and T58A-MYC was PCR amplified and cloned to pLEX vector using Gateway cloning as per the manufacturer's protocol (Thermo Scientific). Infected patient-derived PDAC cells (at multiplicity of infection of 0.5) were briefly selected with puromycin and used at early passages 5–8.

Bioinformatics and statistical analyses

We used AUC to assess the drug's cytotoxicity as described (24). The CellTiter-Glo viability data were normalized using the mean of DMSO control wells on each plate. An open source R package (www.r-project.org) was used to model fitting of dose response curves for each compound using a four-parameter log-logistic formula. The extracted fitted values were used to calculate AUC and to estimate IC_{50} for each compound.

Comparisons between the chemosensitivity of rapid cultures of pancreatic carcinoma cells and the NCI-60 cell lines panel were made using the publicly available data from the CellMiner database (http://discover.nci.nih.gov/cellminer). Using the unique NSC identifying numbers for each compound, 189 CellMiner drugs overlapped with our screening library. Of those, we included in the analysis 156 drugs showing at least 50% cytotoxicity, and for which the data were available in at least 70% of cell lines of the NCI-60 panel. MD-MBA-453 cell line on the NCI-60 panel was excluded from the analysis because it had drug screening data on less than 50% of drugs. Compound activity values were expressed as $-\log_{10}$ and ranked. For data visualization, the hierarchical clustering we used average linkage and distance methods to build heatmaps in R software. We used Student *t* test to analyze the differences between the biological repeats in experiments for statistical significance.

Disclosure of Potential Conflicts of Interest

No potential conflicts of interest were disclosed.

Authors' Contributions

Conception and design: K. Paz, E.A. Golemis, I. Astsaturov

Development of methodology: E. Banina, I.G. Serebriiskii, K. Paz, V. Khazak, I. Astsaturov

Acquisition of data (provided animals, acquired and managed patients, provided facilities, etc.): N. Beglyarova, E. Bobrov, E. Lysenko, N. Skobeleva, L. Gabitova, M. Pressman, J.P. Hoffman, K. Paz, D. Behrens, V. Khazak, S.A. Jablonski, L.M. Weiner, I. Astsaturov

Analysis and interpretation of data (e.g., statistical analysis, biostatistics, computational analysis): N. Beglyarova, E. Banina, Y. Zhou, R. Mukhamadeeva, G. Andrianov, E. Bobrov, K. Paz, V. Khazak, S.A. Jablonski, E.A. Golemis, L.M. Weiner, I. Astsaturov

Writing, review, and/or revision of the manuscript: I.G. Serebriiskii, K. Paz, E.A. Golemis, L.M. Weiner, I. Astsaturov

Administrative, technical, or material support (i.e., reporting or organizing data, constructing databases): D. Restifo, V. Khazak, I. Astsaturov

Study supervision: I. Astsaturov

Other (research conducting): N. Beglyarova

Acknowledgments

We are grateful to the FCCC Cell Culture Facility and Jin Fang for technical assistance with derivation of pancreatic carcinoma cell culture. The authors' work has been supported by the Fox Chase Cancer Center Genomics Facility (Drs. Yuesheng Li and Emmanuelle Nicolas). Champions Oncology Inc. contributed to the data of chemotherapy sensitivity of pancreatic cancer patient-derived xenografts presented in Fig. 2A and Supplementary Fig. S2.

In Memoriam of Dr. Elena Gitelson, a physician and pancreatic cancer patient.

Grant Support

This work was supported by NIH core grant CA-06927, by the Pew Charitable Fund, and by generous gifts from Concetta Greenberg, the Kalargheros family, and from Donald Geary to Fox Chase Cancer Center. Some of the authors were supported by NIH R01 CA188430, K22 CA160725, R21 CA164205, a career development award from Genentech, by Tobacco Settlement funding from the State of Pennsylvania (I. Astsaturov), by a grant from the Bucks County Board of Associates (D. Restifo, L. Gabitova, and I. Astsaturov), R01 CA63366 (E.A. Golemis), by the Program of Competitive Growth of Kazan Federal University (L. Gabitova and I.G. Serebriiskii), and by the grant 15-15-20032 of the Russian Science Foundation (I.G. Serebriiskii, R. Mukhamadeeva, G. Andrianov, and I. Astsaturov) for the bioinformatics analyses of drug sensitivity profiles and RNA expression.

The costs of publication of this article were defrayed in part by the payment of page charges. This article must therefore be hereby marked *advertisement* in accordance with 18 U.S.C. Section 1734 solely to indicate this fact.

Received January 25, 2016; revised May 17, 2016; accepted June 6, 2016; published OnlineFirst July 6, 2016.

References

1. Siegel R, Naishadham D, Jemal A. Cancer statistics, 2012. CA Cancer J Clin 2012;62:10–29.
2. Biankin AV, Waddell N, Kassahn KS, Gingras MC, Muthuswamy LB, Johns AL, et al. Pancreatic cancer genomes reveal aberrations in axon guidance pathway genes. Nature 2012;491:399–405.
3. Waddell N, Pajic M, Patch AM, Chang DK, Kassahn KS, Bailey P, et al. Whole genomes redefine the mutational landscape of pancreatic cancer. Nature 2015;518:495–501.
4. Witkiewicz AK, McMillan EA, Balaji U, Baek G, Lin WC, Mansour J, et al. Whole-exome sequencing of pancreatic cancer defines genetic diversity and therapeutic targets. Nat Commun 2015;6:6744.
5. Cerami E, Gao J, Dogrusoz U, Gross BE, Sumer SO, Aksoy BA, et al. The cBio cancer genomics portal: An open platform for exploring multidimensional cancer genomics data. Cancer Discov 2012;2:401–4.
6. Schleger C, Verbeke C, Hildenbrand R, Zentgraf H, Bleyl U. c-MYC activation in primary and metastatic ductal adenocarcinoma of the pancreas: Incidence, mechanisms, and clinical significance. Mod Pathol 2002;15:462–9.
7. Blumenthal GM, Karuri SW, Zhang H, Zhang L, Khozin S, Kazandjian D, et al. Overall response rate, progression-free survival, and overall survival with targeted and standard therapies in advanced non-small-cell lung cancer: US Food and Drug Administration trial-level and patient-level analyses. J Clin Oncol 2015;33:1008–14.
8. Astsaturov IA, Meropol NJ, Alpaugh RK, Burtness BA, Cheng JD, McLaughlin S, et al. Phase II and coagulation cascade biomarker study of bevacizumab with or without docetaxel in patients with previously treated metastatic pancreatic adenocarcinoma. Am J Clin Oncol 2011;34:70–5.
9. Kim EJ, Sahai V, Abel EV, Griffith KA, Greenson JK, Takebe N, et al. Pilot clinical trial of hedgehog pathway inhibitor GDC-0449 (vismodegib) in combination with gemcitabine in patients with metastatic pancreatic adenocarcinoma. Clin Cancer Res 2014;20:5937–45.
10. Philip PA, Benedetti J, Corless CL, Wong R, O'Reilly EM, Flynn PJ, et al. Phase III study comparing gemcitabine plus cetuximab versus gemcitabine in patients with advanced pancreatic adenocarcinoma: Southwest Oncology Group-directed intergroup trial S0205. J Clin Oncol 2010;28:3605–10.
11. Burris HA3rd, Moore MJ, Andersen J, Green MR, Rothenberg ML, Modiano MR, et al. Improvements in survival and clinical benefit with gemcitabine as first-line therapy for patients with advanced pancreas cancer: A randomized trial. J Clin Oncol 1997;15:2403–13.
12. Moore MJ, Goldstein D, Hamm J, Figer A, Hecht JR, Gallinger S, et al. Erlotinib plus gemcitabine compared with gemcitabine alone in patients with advanced pancreatic cancer: A phase III trial of the National Cancer Institute of Canada Clinical Trials Group. J Clin Oncol 2007;25:1960–6.
13. Von Hoff DD, Ervin T, Arena FP, Chiorean EG, Infante J, Moore M, et al. Increased survival in pancreatic cancer with nab-paclitaxel plus gemcitabine. N Engl J Med 2013;369:1691–703.
14. Conroy T, Desseigne F, Ychou M, Bouché O, Guimbaud R, Bécouarn Y, et al. FOLFIRINOX versus gemcitabine for metastatic pancreatic cancer. N Engl J Med 2011;364:1817–25.
15. Ko AH, Tempero MA, Shan YS, Su WC, Lin YL, Dito E, et al. A multinational phase 2 study of nanoliposomal irinotecan sucrosofate (PEP02, MM-398) for patients with gemcitabine-refractory metastatic pancreatic cancer. Br J Cancer 2013;109:920–5.
16. Voskoglou-Nomikos T, Pater JL, Seymour L. Clinical predictive value of the in vitro cell line, human xenograft, and mouse allograft preclinical cancer models. Clin Cancer Res 2003;9:4227–39.
17. Garralda E, Paz K, López-Casas PP, Jones S, Katz A, Kann LM, et al. Integrated next-generation sequencing and avatar mouse models for personalized cancer treatment. Clin Cancer Res 2014;20:2476–84.
18. Titov DV, Gilman B, He QL, Bhat S, Low WK, Dang Y, et al. XPB, a subunit of TFIIH, is a target of the natural product triptolide. Nat Chem Biol 2011;7:182–8.
19. Liu X, Ory V, Chapman S, Yuan H, Albanese C, Kallakury B, et al. ROCK inhibitor and feeder cells induce the conditional reprogramming of epithelial cells. Am J Pathol 2012;180:599–607.
20. Yuan H, Myers S, Wang J, Zhou D, Woo JA, Kallakury B, et al. Use of reprogrammed cells to identify therapy for respiratory papillomatosis. N Engl J Med 2012;367:1220–7.
21. Kang Y, Zhang R, Suzuki R, Li SQ, Roife D, Truty MJ, et al. Two-dimensional culture of human pancreatic adenocarcinoma cells results in an irreversible transition from epithelial to mesenchymal phenotype. Lab Invest 2015;95:207–22.
22. Abbott A. Neurologists strike gold in drug screen effort. Nature 2002;417:109.
23. Yoo BH, Axlund SD, Kabos P, Reid BG, Schaack J, Sartorius CA, et al. A high-content assay to identify small-molecule modulators of a cancer stem cell population in luminal breast cancer. J Biomol Screen 2012;17:1211–20.
24. Garnett MJ, Edelman EJ, Heidorn SJ, Greenman CD, Dastur A, Lau KW, et al. Systematic identification of genomic markers of drug sensitivity in cancer cells. Nature 2012;483:570–5.
25. Wei G, Margolin AA, Haery L, Brown E, Cucolo L, Julian B, et al. Chemical genomics identifies small-molecule MCL1 repressors and BCL-xL as a predictor of MCL1 dependency. Cancer Cell 2012;21:547–62.
26. Bishton MJ, Harrison SJ, Martin BP, McLaughlin N, James C, Josefsson EC, et al. Deciphering the molecular and biologic processes that mediate histone deacetylase inhibitor-induced thrombocytopenia. Blood 2011;117:3658–68.
27. Cui Y, Brosnan JA, Blackford AL, Sur S, Hruban RH, Kinzler KW, et al. Genetically defined subsets of human pancreatic cancer show unique in vitro chemosensitivity. Clin Cancer Res 2012;18:6519–30.
28. Abaan OD, Polley EC, Davis SR, Zhu YJ, Bilke S, Walker RL, et al. The exomes of the NCI-60 panel: A genomic resource for cancer biology and systems pharmacology. Cancer Res 2013;73:4372–82.
29. Reinhold WC, Sunshine M, Varma S, Doroshow JH, Pommier Y. Using CellMiner 1.6 for systems pharmacology and genomic analysis of the NCI-60. Clin Cancer Res 2015;21:3841–52.
30. Cortes JE, Kantarjian HM, Rea D, Wetzler M, Lipton JH, Akard L, et al. Final analysis of the efficacy and safety of omacetaxine mepesuccinate in patients with chronic- or accelerated-phase chronic myeloid leukemia: Results with 24 months of follow-up. Cancer 2015;121:1637–44.
31. Alberts SR, Foster NR, Morton RF, Kugler J, Schaefer P, Wiesenfeld M, et al. PS-341 and gemcitabine in patients with metastatic pancreatic

adenocarcinoma: A North Central Cancer Treatment Group (NCCTG) randomized phase II study. Ann Oncol 2005;16:1654–61.
32. Chugh R, Sangwan V, Patil SP, Dudeja V, Dawra RK, Banerjee S, et al. A preclinical evaluation of Minnelide as a therapeutic agent against pancreatic cancer. Sci Transl Med 2012;4:156ra139.
33. He QL, Titov DV, Li J, Tan M, Ye Z, Zhao Y, et al. Covalent modification of a cysteine residue in the XPB subunit of the general transcription factor TFIIH through single epoxide cleavage of the transcription inhibitor triptolide. Angew Chem Int Ed Engl 2015;54:1859–63.
34. Lamb J, Crawford ED, Peck D, Modell JW, Blat IC, Wrobel MJ, et al. The connectivity map: Using gene-expression signatures to connect small molecules, genes, and disease. Science 2006;313:1929–35.
35. Vispe S, DeVries L, Créancier L, Besse J, Bréand S, Hobson DJ, et al. Triptolide is an inhibitor of RNA polymerase I and II-dependent transcription leading predominantly to down-regulation of short-lived mRNA. Mol Cancer Ther 2009;8:2780–90.
36. Yeh E, Cunningham M, Arnold H, Chasse D, Monteith T, Ivaldi G, et al. A signalling pathway controlling c-Myc degradation that impacts oncogenic transformation of human cells. Nat Cell Biol 2004;6:308–18.
37. Verma R, Oania R, Fang R, Smith GT, Deshaies RJ. Cdc48/p97 mediates UV-dependent turnover of RNA Pol II. Mol Cell 2011;41:82–92.
38. Inukai N, Yamaguchi Y, Kuraoka I, Yamada T, Kamijo S, Kato J, et al. A novel hydrogen peroxide-induced phosphorylation and ubiquitination pathway leading to RNA polymerase II proteolysis. J Biol Chem 2004;279:8190–5.
39. Wang Y, Lu JJ, He L, Yu Q. Triptolide (TPL) inhibits global transcription by inducing proteasome-dependent degradation of RNA polymerase II (Pol II). PLoS One 2011;6:e23993.
40. Stine ZE, Walton ZE, Altman BJ, Hsieh AL, Dang CV. MYC, metabolism, and cancer. Cancer Discov 2015;5:1024–39.
41. Schlosser I, Hölzel M, Hoffmann R, Burtscher H, Kohlhuber F, Schuhmacher M, et al. Dissection of transcriptional programmes in response to serum and c-Myc in a human B-cell line. Oncogene 2005;24:520–4.
42. Smurnyy Y, Cai M, Wu H, McWhinnie E, Tallarico JA, Yang Y, et al. DNA sequencing and CRISPR-Cas9 gene editing for target validation in mammalian cells. Nat Chem Biol 2014;10:623–5.
43. Gao J, Aksoy BA, Dogrusoz U, Dresdner G, Gross B, Sumer SO, et al. Integrative analysis of complex cancer genomics and clinical profiles using the cBioPortal. Sci Signal 2013;6:pl1.
44. Shain AH, Giacomini CP, Matsukuma K, Karikari CA, Bashyam MD, Hidalgo M, et al. Convergent structural alterations define SWItch/Sucrose NonFermentable (SWI/SNF) chromatin remodeler as a central tumor suppressive complex in pancreatic cancer. Proc Natl Acad Sci U S A 2012;109:E252–9.
45. Tzatsos A, Paskaleva P, Ferrari F, Deshpande V, Stoykova S, Contino G, et al. KDM2B promotes pancreatic cancer via Polycomb-dependent and -independent transcriptional programs. J Clin Invest 2013;123:727–39.
46. Garcia PL, Miller AL, Kreitzburg KM, Council LN, Gamblin TL, Christein JD, et al. The BET bromodomain inhibitor JQ1 suppresses growth of pancreatic ductal adenocarcinoma in patient-derived xenograft models. Oncogene 2016;35:833–45.
47. Mazur PK, Herner A, Mello SS, Wirth M, Hausmann S, Sánchez-Rivera FJ, et al. Combined inhibition of BET family proteins and histone deacetylases as a potential epigenetics-based therapy for pancreatic ductal adenocarcinoma. Nat Med 2015;21:1163–71.
48. Ischenko I, Petrenko O, Hayman MJ. Analysis of the tumor-initiating and metastatic capacity of PDX1-positive cells from the adult pancreas. Proc Natl Acad Sci U S A 2014;111:3466–71.
49. Roy A, McDonald PR, Sittampalam S, Chaguturu R. Open access high throughput drug discovery in the public domain: a Mount Everest in the making. Curr Pharm Biotechnol 2010;11:764–78.
50. Astsaturov I, Ratushny V, Sukhanova A, Einarson MB, Bagnyukova T, Zhou Y, et al. Synthetic lethal screen of an EGFR-centered network to improve targeted therapies. Sci Signal 2010;3:ra67.